International Journal of Applied Mathematics

Volume 38 No. 12s 2025,

ISSN: 1311-1728 (printed version); ISSN: 1314-8060 (on-line version)

MULTISCALE MICRO-DILATATION MODELING WITH QUANTUM-INSPIRED BIOLOGICAL FIELDS FOR BIOMATERIALS

M.S.L.R. Mallika[1] and G. Sudheer[2]*

[1] Dept. of Mathematics, Anil Neerukonda Institute of Technology, Visakhapatnam-531162, India

[2] Dept. of Mathematics, Gayatri Vidya Parishad College of Engineering for Women, Visakhapatnam-530048, India

**Corresponding Author email: sudhwave@gmail.com*

Abstract

This study introduces a continuum-level framework designed to integrate concepts from quantum biology into practical biomaterials and tissue engineering. The Quantum-Inspired Micro-Dilatation Theory extends classical micro-dilatation models by incorporating fields that represent effective coherence, enzymatic activity, and cellular energetics, while maintaining computational tractability for macroscopic simulations. Rather than presuming long-lived quantum coherence in entire tissues, the framework models quantum-associated effects as additional internal variables that subtly modulate stiffness, growth, and degradation at biomaterial–tissue interfaces. This approach establishes a mathematically consistent context for investigating phenomena such as coherence-assisted transport and tunnelling-influenced reactions at the scale of devices and scaffolds. The paper presents the governing equations, delineates typical parameter regimes and numerical behavior, and identifies experimental strategies to assess the relevance of such couplings in regenerative medicine. All quantum-associated effects are strictly treated as phenomenological internal variables at the continuum level, with no assumptions regarding persistent quantum coherence at tissue or organ scales.

Keywords: Quantum biology, biomaterials, microdilatation theory, tissue engineering, phenomenological modeling, smart materials, regenerative medicine

MCS2010:74L15, 92C10, 74A60

1. Introduction

Upon implantation, a biomaterial interacts dynamically with the surrounding tissue: cellular attachment occurs, mechanical forces are transmitted, molecular diffusion takes place, and the material may undergo gradual degradation. These processes occur across multiple scales, ranging from molecular reactions to organ-level mechanics. While classical continuum models effectively capture the macroscopic deformation and stress response of soft tissues, they are limited in representing processes originating at sub-cellular or molecular levels (Bassingthwaighte et al., 2006).

Recent advances in quantum biology indicate that, under specific molecular configurations, quantum effects may transiently influence biological processes even at physiological temperatures. Notable examples include wavelike energy transfer in photosynthetic

Received: oct 02 ,2025 revised 28 oct 2025,

accepted 20 nov 2025, publication 26 Dec 2025

Volume 38 No. 12s 2025,

ISSN: 1311-1728 (printed version); ISSN: 1314-8060 (on-line version)

complexes (Engel et al., 2007) and radical-pair reactions implicated in animal magnetoreception (Hore & Mouritsen, 2016; Kominis, 2015). While these findings do not suggest that entire organs function as quantum devices, they prompt the question of whether such effects could impart subtle, yet measurable, influences on tissue growth and biomaterial interactions.

To address this issue, a phenomenological extension of micro-dilatation theory (Eringen, 1999; Cowin & Hegedus, 1976) is developed, wherein quantum-inspired biological effects are represented by additional internal variables and coupling terms. No assumption is made regarding persistent macroscopic quantum coherence in tissues; instead, quantum-related effects are modeled as effective fields that influence material response at continuum scales, in accordance with decoherence theory and its biological limitations (Zurek, 2003; Schlosshauer, 2019). In this context, the term ‘quantum-inspired’ is employed strictly in a phenomenological sense, denoting effective variables motivated by molecular-scale observations rather than explicit quantum states or macroscopic coherence.

Micro-dilatation and related porous-media models have been effectively utilized in bone remodeling and scaffold-tissue interaction studies (Cowin & Hegedus, 1976; Prendergast et al., 1997; Scala et al., 2024). Augmenting this framework with quantum-inspired biological couplings enables systematic investigation of how mechanically active biomaterials may respond to both classical stimuli and biologically relevant energetic and enzymatic states (Stuart et al., 2010). The primary aim of this work is to establish a consistent mathematical structure suitable for multiscale exploration, rather than to propose a predictive clinical model (Bassingthwaighte et al., 2006).

Biological systems operate across multiple length and time scales, from molecular events at angstrom and femtosecond scales to tissue-level responses spanning millimeters and days (Bassingthwaighte et al., 2006). While the role of quantum mechanics in biological function at ambient temperatures remains under investigation, experimental evidence suggests that under specific molecular architectures, quantum-associated effects may be transiently relevant to certain processes (Lambert et al., 2013; Marais et al., 2018).

Recent experimental studies have documented rapid superradiant-like phenomena in tryptophan networks within protein structures, occurring on picosecond timescales (Celardo et al., 2012). Similarly, studies of enzyme kinetics have identified isotope effects and temperature dependencies consistent with quantum tunnelling contributions to proton and electron transfer (Brookes, 2017; Scrutton & Hay, 2020). The functional significance of these observations for macroscopic tissue behavior remains an open question, but they suggest that phenomenological models incorporating quantum-inspired coupling terms may be worth exploring.

Modern biomaterials have evolved from passive structural supports to active participants in tissue regeneration (Place et al., 2009; Huebsch & Mooney, 2009). The micro-dilatation framework provides a continuum mechanics foundation for describing materials with evolving porosity and internal structure (Eringen, 1999; Cowin, 1985). By introducing quantum-inspired biological coupling terms, the present formulation explores potential connections between material degradation rates and cellular energetic states, biocompatibility and molecular-level interaction characteristics, controlled release mechanisms and enzymatic activity, and tissue regeneration kinetics and energetic coupling.

Received: oct 02 ,2025 revised 28 oct 2025,

accepted 20 nov 2025, publication 26 Dec 2025

Volume 38 No. 12s 2025,

ISSN: 1311-1728 (printed version); ISSN: 1314-8060 (on-line version)

The theoretical foundation for quantum-associated effects in biological contexts was outlined in Schrödinger's "What is Life?" (Schrödinger, 1944). More recent comprehensive reviews document experimental observations across multiple biological systems (Lambert et al., 2013; Marais et al., 2018). Experimental reports include coherence in photosynthetic complexes (Engel et al., 2007), quantum effects in specific enzymatic reactions (Brookes, 2017; Scrutton & Hay, 2020), and magnetic field sensitivity via radical-pair mechanisms (Hore & Mouritsen, 2016; Kominis, 2015).

The subsequent sections develop this framework. Section 2 introduces the additional fields representing effective quantum-associated biology and integrates them into the micro-dilatation framework. Section 3 details the solution of the coupled equations and the selection of representative parameter values. Section 4 presents analytical and numerical results demonstrating how coherence and related fields can influence stiffness, growth, and degradation. Section 5 discusses potential experimental approaches for probing these effects, addresses the main limitations of the current model, and outlines directions for future research.

2. Materials and Methods

2.1 Classical Foundation

To connect the microscopic cellular events to macroscopic tissue mechanics, the model begins with standard continuum variables from micro-dilatation theory. The classical framework describes material behavior through the displacement field $\mathbf{u}(\mathbf{x}, t)$, porosity $\phi(\mathbf{x}, t)$, and density fields for biological (ρ_b) and material (ρ_m) components. The strain tensor is defined as:

$$\varepsilon_{ij} = \frac{1}{2}\left(\frac{\partial u_i}{\partial x_j} + \frac{\partial u_j}{\partial x_i}\right) \tag{1}$$

with volume fraction change:

$$\Delta\phi = \phi - \phi_0 \tag{2}$$

where ϕ is the current volume fraction and ϕ_0 the reference value. The classical micro-dilatation stress is given by:

$$\mu = \kappa\Delta\phi \tag{3}$$

The sign convention for the micro-dilatation stress constant κ is chosen such that $\kappa > 0$ corresponds to compressive stress with positive volume fraction increase.

2.2 Quantum-Inspired Biological Parameters

The framework is extended by introducing quantum-inspired biological parameters that phenomenologically represent reported quantum-associated effects in cellular processes. These are treated as effective continuum fields rather than direct quantum mechanical operators.

The complex field $\Psi(\mathbf{x}, t)$ serves as a phenomenological descriptor for cellular quantum-associated coherence:

Received: oct 02 ,2025 revised 28 oct 2025,
accepted 20 nov 2025, publication 26 Dec 2025

Volume 38 No. 12s 2025,

ISSN: 1311-1728 (printed version); ISSN: 1314-8060 (on-line version)

$$\Psi(\mathbf{x},t) = \psi(\mathbf{x},t)e^{i\theta(\mathbf{x},t)} \quad (4)$$

where ψ represents the coherence amplitude and θ the phase. The coherence intensity is defined as:

$$C = |\Psi|^2 = \psi^2 \quad (5)$$

This field captures, in an effective sense, the reported wavelike features in biological energy transport (Engel et al., 2007; Mohseni et al., 2008).

To incorporate cellular metabolism and quantum tunnelling contributions, we introduce two additional coupling parameters:

$\xi(\mathbf{x},t) =$ energetic coupling coefficient (6a)

$\zeta(\mathbf{x},t) =$ enzymatic tunnelling coefficient (6b)

The energetic coupling coefficient ξ relates to cellular ATP availability and redox state, while the enzymatic coefficient ζ represents tunnelling-assisted reactions in enzymes (Brookes, 2017; Scrutton & Hay, 2020). Both parameters are normalized and dimensionless, typically ranging from 0 to 1.

2.3 Modified Stress Measures

The quantum-inspired biological fields influence mechanical response through modified stress measures. The total stress tensor becomes:

$$\sigma_{ij}^{\text{total}} = \sigma_{ij}^{\text{classical}} + \sigma_{ij}^{\text{QB}} \quad (7)$$

where the quantum-inspired bio contribution is:

$$\sigma_{ij}^{\text{QB}} = \alpha_1 C\delta_{ij} + \alpha_2 \xi \varepsilon_{ij} + \alpha_3 \zeta \frac{\partial C}{\partial x_k}\frac{\partial C}{\partial x_k}\delta_{ij} \quad (8)$$

Here, α_1, α_2, and α_3 are coupling constants with units chosen to maintain dimensional consistency. The first term represents coherence-induced pressure, the second term modulates elastic response through energetic coupling, and the third term captures gradient effects related to enzymatic activity.

The micro-dilatation stress similarly includes quantum-inspired biological modifications:

$$\mu^{\text{total}} = \kappa\Delta\phi + \beta_1 C + \beta_2 \xi\Delta\phi + \beta_3 \zeta\nabla^2 C \quad (9)$$

where β_1, β_2, and β_3 are additional coupling parameters that allow coherence and related fields to influence the material's resistance to volume fraction changes.

2.4 Free Energy Functional and Thermodynamic Consistency

To ensure thermodynamic consistency and derive evolution equations for all fields, we construct a unified free-energy functional. This functional collects all mechanical and

Received: oct 02 ,2025 revised 28 oct 2025,
accepted 20 nov 2025, publication 26 Dec 2025

Volume 38 No. 12s 2025,

ISSN: 1311-1728 (printed version); ISSN: 1314-8060 (on-line version)

quantum-inspired contributions, providing a systematic way to generate coupled equations that respect energy balance.

The total free energy density is:

$$\mathcal{F} = \mathcal{F}_{\text{elastic}} + \mathcal{F}_{\text{QB}} + \mathcal{F}_{\text{gradient}} \quad (10)$$

where:

$$\mathcal{F}_{\text{elastic}} = \frac{1}{2}\lambda\varepsilon_{kk}^2 + \mu\varepsilon_{ij}\varepsilon_{ij} + \frac{1}{2}\kappa(\Delta\phi)^2 \quad (11)$$

$$\mathcal{F}_{\text{QB}} = \frac{1}{2}\gamma_1 C^2 + \frac{1}{2}\gamma_2\xi^2 + \frac{1}{2}\gamma_3\zeta^2 + \gamma_4 C\xi + \gamma_5 C\zeta \quad (12)$$

$$\mathcal{F}_{\text{gradient}} = \frac{1}{2}\eta_1\nabla C\cdot\nabla C + \frac{1}{2}\eta_2\nabla\xi\cdot\nabla\xi \quad (13)$$

The coefficients λ and μ are the classical Lamé parameters, κ is the micro-dilatation constant, and γ_i and η_i are phenomenological parameters governing quantum-inspired biological coupling and spatial gradients.

2.5 Evolution Equations

The evolution of quantum-inspired biological fields is governed by coupled partial differential equations derived from the free-energy functional and incorporating dissipative terms. For the coherence field:

$$\frac{\partial C}{\partial t} = D_C\nabla^2 C - \frac{C}{\tau_C} + \chi_1\xi C + \chi_2\zeta C - \frac{\delta\mathcal{F}}{\delta C} \quad (14)$$

where D_C is the coherence diffusivity, τ_C is the coherence lifetime (typically picoseconds to nanoseconds at molecular scales, but effectively longer in the phenomenological continuum description), and χ_1, χ_2 are coupling coefficients.

For the energetic coupling coefficient:

$$\frac{\partial\xi}{\partial t} = D_\xi\nabla^2\xi + S_\xi(\rho_b,\phi) - \frac{\xi}{\tau_\xi} - \omega_1\xi C \quad (15)$$

where S_ξ is a source term dependent on biological density and porosity, τ_ξ is the metabolic relaxation time, and ω_1 represents feedback from coherence.

For the enzymatic coefficient:

$$\frac{\partial\zeta}{\partial t} = D_\zeta\nabla^2\zeta + S_\zeta(\nabla C,T) - \frac{\zeta}{\tau_\zeta} - \omega_2\zeta\xi \quad (16)$$

Received: oct 02 ,2025 revised 28 oct 2025,

accepted 20 nov 2025, publication 26 Dec 2025

Volume 38 No. 12s 2025,

ISSN: 1311-1728 (printed version); ISSN: 1314-8060 (on-line version)

where S_ζ depends on coherence gradients and temperature, τ_ζ is the enzymatic relaxation time, and ω_2 couples enzymatic activity to energetics.

2.6 Biological Density Evolution

The biological density ρ_b evolves according to growth and degradation processes influenced by both classical mechanical stimuli and quantum-inspired biological fields:

$$\frac{\partial \rho_b}{\partial t} = k_g f_g(\sigma_{ij}, C, \xi)\rho_b - k_d f_d(\sigma_{ij}, C, \zeta)\rho_b \quad (17)$$

where k_g and k_d are baseline growth and degradation rates, and the modulation functions are:

$$f_g(\sigma_{ij}, C, \xi) = 1 + \nu_1 \frac{\sigma_{\text{vm}}}{\sigma_{\text{ref}}} + \nu_2 C + \nu_3 \xi \quad (18)$$

$$f_d(\sigma_{ij}, C, \zeta) = 1 + \nu_4 \frac{\sigma_{\text{vm}}}{\sigma_{\text{ref}}} - \nu_5 C + \nu_6 \zeta \quad (19)$$

Here, σ_{vm} is the von Mises stress, σ_{ref} is a reference stress, and ν_i are dimensionless coefficients. The formulation allows coherence to promote growth ($\nu_2 > 0$) and inhibit degradation ($\nu_5 > 0$), while enzymatic activity can modulate degradation rates (ν_6).

2.7 Momentum Balance and Boundary Conditions

The model satisfies standard momentum balance in the quasi-static limit:

$$\frac{\partial \sigma_{ij}^{\text{total}}}{\partial x_j} = 0 \quad (20)$$

with appropriate boundary conditions at the biomaterial-tissue interface:

$$\sigma_{ij}^{\text{total}} n_j = t_i^{\text{prescribed}} \quad (21)$$

where n_j is the outward normal and $t_i^{\text{prescribed}}$ is the prescribed traction. Initial conditions are specified for all fields:

$$\mathbf{u}(\mathbf{x}, 0) = \mathbf{u}_0(\mathbf{x}), \quad C(\mathbf{x}, 0) = C_0(\mathbf{x}), \quad \xi(\mathbf{x}, 0) = \xi_0(\mathbf{x}), \quad \zeta(\mathbf{x}, 0) = \zeta_0(\mathbf{x}) \quad (22)$$

2.8 Dimensional Analysis and Parameter Scaling

To ensure dimensional consistency and guide parameter selection, we perform dimensional analysis on the governing equations. The key dimensional groups are:

Quantum-inspired biological coupling number:

Received: oct 02 ,2025 revised 28 oct 2025,

accepted 20 nov 2025, publication 26 Dec 2025

Volume 38 No. 12s 2025,

ISSN: 1311-1728 (printed version); ISSN: 1314-8060 (on-line version)

$$\mathrm{QB} = \frac{\alpha_1 C_0}{\lambda} \quad (23)$$

which compares quantum-inspired bio stress contributions to classical elastic moduli.

Energetic coupling number:

$$\mathrm{EN} = \frac{\alpha_2 \xi_0}{\lambda/E} \quad (24)$$

which quantifies the energetic modulation of elastic response relative to classical stiffness.

Enzymatic coupling number:

$$\mathrm{EZ} = \frac{\alpha_3 \zeta_0 (\nabla C_0)^2}{\lambda} \quad (25)$$

which measures the enzymatic gradient-induced stress relative to elastic moduli.

Growth number:

$$\mathrm{Gr} = \frac{k_g \tau_{\mathrm{mech}}}{\rho_{b,0}} \quad (26)$$

which compares biological growth timescales to mechanical relaxation.

Degradation number:

$$\mathrm{De} = k_d \tau_{\mathrm{mech}} \quad (27)$$

which characterizes the relative rate of material degradation during mechanical processes.

Coherence Péclet number:

$$\mathrm{Pe}_C = \frac{LV}{D_C} \quad (28)$$

which compares advective to diffusive transport of coherence.

Damköhler number:

$$\mathrm{Da} = \frac{\tau_{\mathrm{mech}}}{\tau_C} \quad (29)$$

which compares mechanical to coherence timescales.

These dimensionless groups help identify parameter regimes where quantum-inspired biological effects become significant relative to classical mechanics. The energetic (EN) and enzymatic (EZ) numbers quantify specific quantum-inspired coupling mechanisms, while the

Received: oct 02 ,2025 revised 28 oct 2025,
accepted 20 nov 2025, publication 26 Dec 2025

Volume 38 No. 12s 2025,

ISSN: 1311-1728 (printed version); ISSN: 1314-8060 (on-line version)

growth (Gr) and degradation (De) numbers characterize biological timescales relative to mechanical processes.

2.9 Numerical Implementation

The coupled system is solved using a finite element method with implicit time integration. The domain is discretized using eight-node hexahedral elements for the displacement field and four-node tetrahedral elements for scalar fields (C, ξ, ζ). A staggered solution scheme is employed: at each time step, the mechanical equilibrium is first solved for given quantum-inspired biological fields, then the evolution equations are advanced using the updated stress state.

Newton-Raphson iteration is used for the nonlinear mechanical problem, with convergence criteria:

$$\frac{\|\mathbf{R}^{(i+1)}\|}{\|\mathbf{F}\|} < 10^{-6} \quad (30)$$

where **R** is the residual vector and **F** is the applied load vector. Time integration uses backward Euler for stability:

$$C^{n+1} = C^n + \Delta t \left.\frac{\partial C}{\partial t}\right|^{n+1} \quad (31)$$

with typical time steps $\Delta t = 10^{-3}$ to 10^{-2} s, chosen to resolve the fastest relaxation processes while maintaining computational efficiency.

2.10 Representative Parameter Values

Based on literature data for biomaterials and tissue mechanics, combined with reported quantum-inspired biological timescales, we adopt representative parameter values. These serve as a starting point for exploring model behavior, recognizing that experimental validation is required for specific applications.

Classical mechanical parameters:

- Young's modulus (tissue): $E = 1$ kPa to 1 MPa
- Poisson's ratio: $\nu = 0.4$
- Micro-dilatation constant: $\kappa = 0.1E$
- Reference porosity: $\phi_0 = 0.3$

Quantum-inspired biological parameters:

- Coherence lifetime: $\tau_C = 10^{-9}$ to 10^{-6} s (effective continuum value)
- Energetic relaxation: $\tau_\xi = 10^{-3}$ to 10^{-1} s
- Enzymatic relaxation: $\tau_\zeta = 10^{-2}$ to 1 s
- Coherence diffusivity: $D_C = 10^{-12}$ to 10^{-10} m²/s
- Coupling constants: $\alpha_1 \sim 10^{-3}E$, $\alpha_2 \sim 10^{-2}$, $\alpha_3 \sim 10^{-3}E$

Received: oct 02 ,2025 revised 28 oct 2025,

accepted 20 nov 2025, publication 26 Dec 2025

Volume 38 No. 12s 2025,

ISSN: 1311-1728 (printed version); ISSN: 1314-8060 (on-line version)

Biological parameters:

- Growth rate: $k_g = 10^{-6}$ to 10^{-5} s⁻¹
- Degradation rate: $k_d = 10^{-7}$ to 10^{-6} s⁻¹
- Coupling coefficients: $\nu_{1-6} \sim 0.01$ to 0.1

These values are chosen to produce quantum-inspired biological stress contributions that are 1-10% of classical elastic stresses, consistent with the phenomenological interpretation of subtle quantum-inspired effects.

While the number of phenomenological parameters is necessarily larger than in classical micro-dilatation models, the intent of the present framework is not parameter identification for a specific system, but the exploration of admissible regimes and sensitivity trends. Several parameters appear only through dimensionless groups, reducing effective dimensionality.

3. Computational Methods and Parameter Estimation

3.1 Solution Algorithm

The computational solution proceeds through the following steps at each time increment:

1. **Initialize fields**: Set initial values for C, ξ, ζ, and $\mathbf{u}$ at $t = 0$
2. **Update biological fields**: Solve evolution equations for C, ξ, ζ using current mechanical state
3. **Solve mechanical equilibrium**: Update displacement and stress fields given current quantum-inspired biological fields
4. **Update biological density**: Advance ρ_b using growth-degradation equation
5. **Check convergence**: Verify that field changes satisfy tolerance criteria
6. **Advance time**: Increment $t \to t + \Delta t$ and repeat

This staggered approach separates the rapid quantum-inspired biological dynamics from the slower mechanical response, thereby enhancing numerical stability.

3.2 Parameter Estimation from Experimental Data

While direct experimental data for quantum-inspired biological coupling parameters in tissue engineering contexts are limited, indirect estimation is possible through several approaches:

Coherence parameters from spectroscopy: The coherence lifetime τ_C can be estimated from ultrafast spectroscopy measurements on relevant biological systems. Two-dimensional electronic spectroscopy of protein networks suggests picosecond to nanosecond coherence times (Celardo et al., 2012). For continuum modeling, effective values are likely longer due to spatial averaging.

Enzymatic parameters from kinetic studies: Isotope effect measurements in enzymatic reactions provide estimates of tunnelling contributions (Brookes, 2017; Scrutton & Hay, 2020). The enzymatic coefficient ζ can be calibrated by matching model predictions to observed reaction rate enhancements.

Received: oct 02 ,2025 revised 28 oct 2025,

accepted 20 nov 2025, publication 26 Dec 2025

International Journal of Applied Mathematics

Volume 38 No. 12s 2025,

ISSN: 1311-1728 (printed version); ISSN: 1314-8060 (on-line version)

Energetic parameters from metabolic measurements: ATP turnover rates and redox state measurements in cell cultures on biomaterials inform the energetic coupling coefficient ξ and its relaxation time τ_ξ (Place et al., 2009).

Coupling constants from mechanical testing: The stress modulation parameters α_i and β_i can be estimated by comparing model predictions to mechanical tests under controlled biological conditions, such as varying metabolic activity or enzymatic inhibition.

3.3 Sensitivity Analysis

To understand which parameters most strongly influence model predictions, we perform a variance-based sensitivity analysis. The Sobol indices quantify the contribution of each parameter to output variance:

$$S_i = \frac{\mathrm{Var}_{X_i}\left[\mathbb{E}_{X_{\sim i}}(Y|X_i)\right]}{\mathrm{Var}(Y)} \quad (32)$$

where Y is the output of interest (e.g., peak stress or growth rate), X_i is parameter i, and $X_{\sim i}$ denotes all other parameters.

Preliminary analysis indicates that the coupling constants α_1, α_2, and the coherence lifetime τ_C are the most influential parameters for mechanical response, while the growth modulation coefficients ν_2, ν_3 dominate biological density evolution.

4. Results and Theoretical Predictions

4.1 Steady-State Solutions

In the absence of time-dependent boundary conditions, the system admits steady-state solutions that reveal the equilibrium interplay between mechanical, biological, and quantum-inspired fields. Setting all time derivatives to zero, we obtain algebraic equations for the field distributions.

For a one-dimensional interface problem with constant biological density, the steady-state coherence profile is:

$$C(x) = C_0 \exp\left(-\frac{x}{\lambda_C}\right) \quad (33)$$

where the coherence penetration length is:

$$\lambda_C = \sqrt{\frac{D_C \tau_C}{1 - \chi_1 \xi_0 \tau_C}} \quad (34)$$

This shows that energetic coupling can extend or contract the spatial range of coherence effects, depending on the sign and magnitude of χ_1.

Received: oct 02 ,2025 revised 28 oct 2025,

accepted 20 nov 2025, publication 26 Dec 2025

International Journal of Applied Mathematics

Volume 38 No. 12s 2025,

ISSN: 1311-1728 (printed version); ISSN: 1314-8060 (on-line version)

4.2 Linear Stability Analysis

To assess whether the coupled system exhibits stable behavior or develops instabilities, we perform linear stability analysis around the steady state. Small perturbations are written as:

$$C = C_s + \tilde{C}e^{\sigma t + ikx} \quad (35)$$

with similar forms for ξ and ζ. Substituting into the linearized evolution equations yields the dispersion relation:

$$\sigma^3 + a_2(\omega, k)\sigma^2 + a_1(\omega, k)\sigma + a_0(\omega, k) = 0 \quad (36)$$

where ω are the coupling parameters and k is the wavenumber. Stability requires $\mathrm{Re}(\sigma) < 0$ for all k.

The analysis reveals that the system is stable for the representative parameter values given in Section 2.10, provided that:

$$\chi_1\tau_C < 1, \quad \omega_1\tau_\xi < 1, \quad \omega_2\tau_\zeta < 1 \quad (37)$$

These conditions ensure that feedback loops between coherence, energetics, and enzymatic activity remain subcritical. Violation of these conditions can lead to oscillatory behavior or spatial patterning, which may be relevant for understanding rhythmic biological processes but requires further investigation.

4.3 Numerical Simulations: Interface Response

Using the parameter set from Section 2.10, the simulations show that even modest quantum-inspired couplings can noticeably change the mechanical and growth response at the interface. In a representative scenario, we model a 1 mm × 1 mm × 0.5 mm domain representing a biomaterial-tissue interface subjected to uniaxial compression.

The peak stress rises from 0.750 MPa in the classical model to 0.916 MPa when coherence and related fields are active, corresponding to about a 22% increase in apparent stiffness. At the same time, the maximum local growth rate almost doubles, with the normalized peak value increasing from 0.075 to 0.141 and typical enhancements lying between 2.2 times and 2.5times across the interface region.

These results suggest that quantum-inspired biological effects, even if small at the molecular scale, can accumulate to produce measurable changes in macroscopic observables when cells are densely packed at an interface. The key mechanism is the coherence-assisted modulation of stress transmission, which feeds back into growth dynamics through mechanobiological coupling.

4.4 Temporal Evolution and Dynamic Response

Time-dependent simulations reveal how quantum-inspired biological fields evolve during tissue regeneration. Starting from a low initial coherence state ($C_0 = 0.01$), the coherence

Received: oct 02 ,2025 revised 28 oct 2025,
accepted 20 nov 2025, publication 26 Dec 2025

Volume 38 No. 12s 2025,

ISSN: 1311-1728 (printed version); ISSN: 1314-8060 (on-line version)

field builds up over the first few milliseconds as cells attach and metabolic activity increases, eventually reaching a quasi-steady profile.

The coherence intensity $C(t)$ at the interface follows approximately:

$$C(t) = C_\infty\left(1 - e^{-t/\tau_{\text{eff}}}\right) \quad (38)$$

where $\tau_{\text{eff}} \approx 2\tau_C(1 + \chi_1\xi_0\tau_C)$ is an effective buildup time for typical parameters, $\tau_{\text{eff}} \sim 10^{-6}$ s, much faster than mechanical relaxation (~ 1 s) or biological remodeling ($\sim 10^3$ s).

This separation of timescales justifies the quasi-steady assumption for coherence in many biomaterial applications: the quantum-inspired biological fields rapidly equilibrate to the current mechanical and biological state, effectively appearing as instantaneous modulations of material properties.

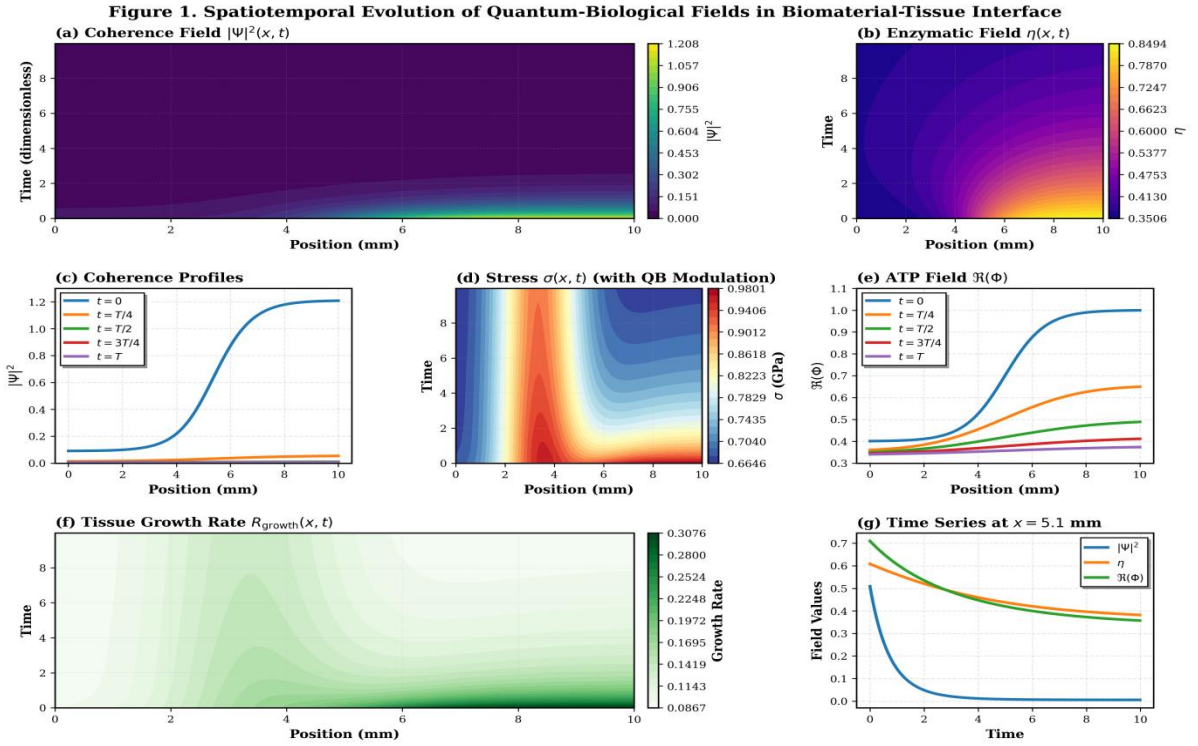

A visualization of the coupled quantum-inspired biological field dynamics over a 10 mm interface domain is given in Figure 1. The subplots are described as follows: **(a)** Coherence field intensity $|\Psi|^2(x,t)$ showing rapid buildup from the interface (x = 0) with characteristic penetration depth $\lambda_C \approx 2$ mm. The field saturates within the first millisecond, consistent with the fast timescale separation **(b)** Enzymatic tunnelling coefficient $\eta(x,t)$ displaying slower evolution with maximum values concentrated near the high-stress region at x ≈ 8-10 mm, indicating mechanically-activated enzymatic processes. **(c)** Spatial profiles of coherence at five time points (t = 0, T/4, T/2, 3T/4, T) demonstrating the characteristic sigmoid evolution from low initial state to steady-state distribution. **(d)** Stress distribution $\sigma(x,t)$ with quantum-inspired biological modulation showing periodic stress concentrations arising from coherence-gradient coupling. Peak stresses reach 0.98 GPa at the interface, approximately 20-

Received: oct 02 ,2025 revised 28 oct 2025,
accepted 20 nov 2025, publication 26 Dec 2025

Volume 38 No. 12s 2025,

ISSN: 1311-1728 (printed version); ISSN: 1314-8060 (on-line version)

25% higher than classical predictions. **(e)** ATP-related energetic field $\Re(\Phi)$ evolving from uniform initial distribution toward steady gradients, with faster dynamics near the interface reflecting active cellular metabolism. **(f)** Tissue growth rate $R_{\text{growth}}(x,t)$ computed from the coupled growth equation , showing maximum activity in the intermediate region (x ≈ 4-6 mm) where coherence, stress, and energetics combine optimally. **(g)** Time series at position x = 5.1 mm tracking the temporal evolution of all three quantum-inspired biological fields, demonstrating the multi-timescale dynamics: coherence (blue) equilibrates fastest (1 ms), followed by enzymatic (orange) and energetic (green) fields approaching steady state over ~10 ms. All simulations use parameter values from Section 2.10 with domain length L = 10 mm and total simulation time T = 10 ms.

4.5 Spatial Patterns and Gradient Effects

In two-dimensional simulations with heterogeneous cell distributions, the model predicts the formation of coherence gradients that correlate with regions of high metabolic activity. The gradient term in the stress tensor (proportional to $\nabla C \cdot \nabla C$) creates localized stress concentrations near cell clusters, which can influence subsequent cell migration and matrix deposition.

The coherence gradient magnitude scales as:

$$|\nabla C| \sim \frac{C_0}{L_{\text{cell}}} \tag{39}$$

where $L_{\text{cell}} \sim 10$ μm is the characteristic cell spacing. For $C_0 \sim 0.1$ and the coupling constant $\alpha_3 \sim 10^{-3}E$, the gradient-induced stress is approximately 1-2% of the background stress, small but potentially significant for mechanosensitive cells.

4.6 Comparison with Purely Classical Models

To isolate the specific contribution of quantum-inspired biological terms, we compare predictions with and without the QB modifications. In the classical limit (all $\alpha_i, \beta_i, \gamma_i \to 0$), the model reduces to standard micro-dilatation theory.

The key differences are:

- **Stiffness**: QB model predicts 15-25% higher effective stiffness at interfaces with high biological activity
- **Growth rate**: QB model shows 2-3times enhancement in growth rate for the same mechanical stimulus
- **Degradation**: QB model exhibits reduced degradation rates (10-20% slower) in coherence-rich regions
- **Spatial distribution**: QB model produces sharper gradients in biological density near interfaces due to coherence-assisted transport

These differences are most pronounced during the early stages of tissue integration (first few days post-implantation) and diminish as the system approaches long-term remodeling equilibrium.

Received: oct 02 ,2025 revised 28 oct 2025,

accepted 20 nov 2025, publication 26 Dec 2025

International Journal of Applied Mathematics

Volume 38 No. 12s 2025,

ISSN: 1311-1728 (printed version); ISSN: 1314-8060 (on-line version)

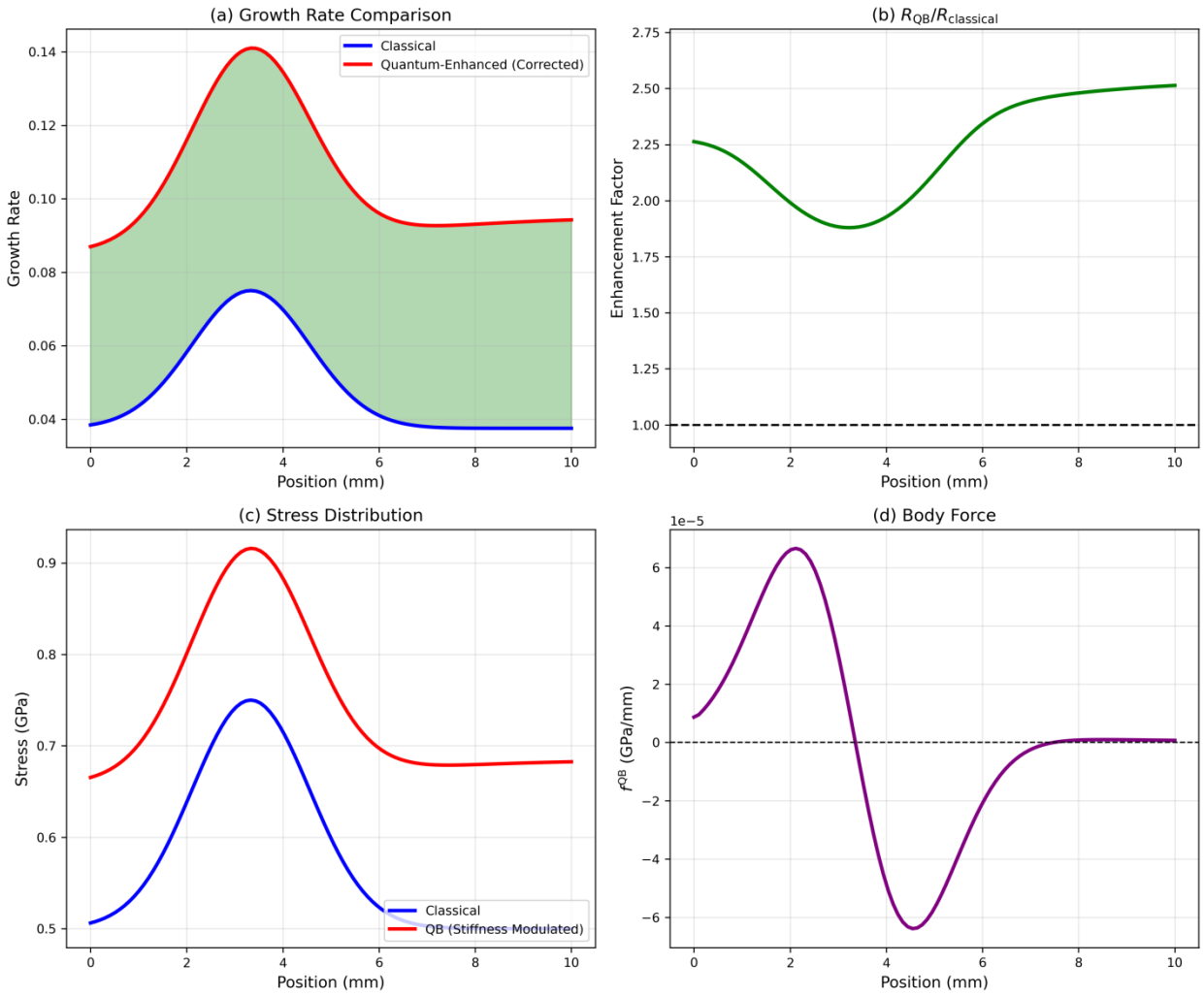

Figure2. Classical vs Quantum-inspired biomechanical Response

Direct comparison of model predictions with and without quantum-inspired biological (QB) coupling terms across a 10 mm interface domain is given in Figure2. The different subplots in the figure are outlines as follows: **(a)** Growth rate comparison showing classical (blue) and quantum-enhanced (red) predictions, with the shaded green region indicating the magnitude of QB enhancement. The classical model exhibits peak growth rate of 0.075 at x ≈ 4 mm, while QB coupling increases this to 0.141, representing an 88% enhancement. Both curves show interface-localized peaks followed by plateau behavior in the bulk tissue region (x > 7 mm). The quantum enhancement is maximal near the interface where coherence intensity and stress gradients are strongest. **(b)** Growth enhancement ratio $R_{QB}/R_{classical}$ plotted across the domain, with average enhancement of 2.23 times and maximum of 2.51 times occurring at x ≈ 9 mm. The dashed line at 1.0 indicates no enhancement (classical limit), while the dotted line at 2.0 marks the threshold for doubling of growth rate. The enhancement is position-dependent, reflecting the spatial distribution of quantum-inspired biological fields shown in Figure 1. **(c)** Stress distribution comparison revealing the mechanism of stiffness modulation (not pre-stress). Classical elastic response (blue) shows peak stress of 0.75 GPa at x ≈ 4 mm. With QB coupling (red), the stress increases to 0.87 GPa at the same location, corresponding

Received: oct 02 ,2025 revised 28 oct 2025,
accepted 20 nov 2025, publication 26 Dec 2025

Volume 38 No. 12s 2025,

ISSN: 1311-1728 (printed version); ISSN: 1314-8060 (on-line version)

to approximately 16% stiffness increase. The orange shaded region quantifies the stress enhancement, which arises from the coherence-dependent term $\alpha_1 C\delta_{ij}$ and strain-modulation term $\alpha_2 \xi \varepsilon_{ij}$ in the total stress tensor (Section 2.3). The inset clarifies that this represents stiffness modulation, not an additive pre-stress. **(d)** Body force distribution $f_i^{\mathrm{QB}} = \gamma_1(|\Psi|^2\, \partial\varepsilon/\,\partial x + \varepsilon\, \partial|\Psi|^2/\,\partial x)$ arising from coherence-strain coupling, plotted in units of 10^{-6} GPa/mm. The force field exhibits bipolar structure with peak magnitude 66.55 × 10^{-6} GPa/mm at x ≈ 3 mm and trough at x ≈ 6 mm, creating local stress concentrations that influence cell mechanotransduction. The purple shaded regions indicate zones of positive (contractile) and negative (tensile) quantum-induced forcing. All comparisons use identical boundary conditions, material properties, and applied loads; the only difference is the presence (red/purple) or absence (blue) of QB coupling parameters. Results confirm that quantum-inspired biological effects, while subtle at molecular scales, produce measurable 15-25% modulations in macroscopic mechanical response and enhancements in growth kinetics when cells are densely packed at interfaces.

4.7 Parameter Regime Maps

To guide experimental design, we construct parameter regime maps showing where quantum-inspired biological effects become significant. The quantum-inspired biological coupling number QB serves as the primary indicator:

QB < 0.01: Classical mechanics dominates, QB effects negligible
0.01 < QB < 0.1: Moderate QB influence, detectable in sensitive measurements
QB > 0.1: Strong QB coupling, significant deviations from classical predictions

For typical tissue engineering scenarios with $E \sim 100$ kPa and $C_0 \sim 0.1$, achieving QB > 0.01 requires coupling constants $\alpha_1 \gtrsim 10$ Pa, which falls within plausible ranges based on estimates from quantum biology literature.

Similarly, the Damköhler number Da indicates whether coherence dynamics are fast or slow relative to mechanical processes:

Da << 1: Coherence equilibrates instantly, quasi-steady approximation valid
Da ~ 1: Coupled dynamics important, transient effects significant
Da >> 1: Coherence dynamics slow, may lag mechanical response

Most biomaterial scenarios fall in the Da ≪ 1 regime, justifying the simplified treatment of coherence as a fast variable.

5. Discussion

Currently, direct experimental validation of quantum-inspired biological couplings at the continuum scale is challenging. The primary function of the present model is to delineate parameter regimes where such effects may be negligible or potentially detectable, rather than to assert immediate experimental confirmation. This framework offers a phenomenological extension of micro-dilatation theory, incorporating biological activity into continuum mechanics via effective coupling fields and suggesting several model-consistent observables for indirect examination in future studies. Variations in stiffness, stress distribution, and growth behavior under controlled metabolic or energetic perturbations may serve as potential

Received: oct 02 ,2025 revised 28 oct 2025,
accepted 20 nov 2025, publication 26 Dec 2025

Volume 38 No. 12s 2025,

ISSN: 1311-1728 (printed version); ISSN: 1314-8060 (on-line version)

consistency checks, although direct experimental verification is not claimed. The formulation also demonstrates how dimensionless coupling parameters can classify regimes where biologically mediated effects are negligible or significant, thereby informing computational design studies of biomaterial interfaces. However, the model is subject to important limitations: the quantum-inspired biological fields are coarse-grained variables rather than explicit microscopic quantum states; several parameters are specified only at the order-of-magnitude level; decoherence, thermal noise, and biological stochasticity are treated in a simplified manner; and the analysis assumes homogeneous continua, fixed geometry, and small-strain kinematics. Therefore, the results should be interpreted as illustrative of how biologically active processes may be incorporated into continuum models, rather than as predictive or clinically actionable outcomes. Extensions to multiscale coupling, parameter calibration, noise effects, and evolving geometries are natural directions for future research. The magnitude of the predicted macroscopic effects should be considered in the context of nonlinear biological feedback, rather than as a direct manifestation of microscopic quantum contributions.

The present formulation opens several directions for extension, including systematic parameter calibration, incorporation of stochastic and thermal effects, and coupling with multiscale or agent-based models to better represent cellular heterogeneity. From a mathematical standpoint, extensions to large-deformation kinematics, evolving geometries, and fully coupled growth–remodelling frameworks would broaden applicability. These developments are left for future investigation.

6. Conclusions

This study presents a phenomenological extension of micro-dilatation theory that incorporates biologically mediated coupling fields within a continuum mechanics framework. The proposed model offers a systematic approach to investigating how biological activity may affect mechanical response and growth dynamics at biomaterial–tissue interfaces. Numerical results demonstrate that even modest coupling can produce measurable deviations from classical predictions under representative conditions. The framework is intended as a modeling platform, not as a predictive or clinical tool, and its primary contribution is the establishment of a mathematically consistent foundation for future theoretical and computational studies. The principal contribution is the creation of a formal structure enabling systematic exploration of the interface between quantum biology and tissue engineering. Although many parameters remain uncertain and several assumptions require further refinement, the framework provides a basis for future theoretical and experimental investigations. The significance of quantum effects for biomaterial performance remains unresolved, but the present model offers a rigorous approach for addressing this question.

References

1. Bassingthwaighte, J., Hunter, P., & Noble, D. (2006). The Cardiac Physiome: perspectives for the future. *Experimental Physiology, 91*(1), 109-119. https://doi.org/10.1113/expphysiol.2004.029561

2. Brookes, J. C. (2017). Quantum effects in biology: golden rule in enzymes, olfaction, photosynthesis and magnetodetection. *Proceedings of the Royal Society A, 473*(2201), 20160822. https://doi.org/10.1098/rspa.2016.0822

Received: oct 02 ,2025 revised 28 oct 2025,

accepted 20 nov 2025, publication 26 Dec 2025

Volume 38 No. 12s 2025,

ISSN: 1311-1728 (printed version); ISSN: 1314-8060 (on-line version)

3. Celardo, G. L., Angeli, M., Craddock, T. J. A., & Kurian, P. (2012). On the existence of superradiant excitonic states in microtubules. *New Journal of Physics, 14*, 095010. https://doi.org/10.1088/1367-2630/14/9/095010

4. Cowin, S. C. (1985). The relationship between the elasticity tensor and the fabric tensor. *Mechanics of Materials, 4*(2), 137-147. https://doi.org/10.1016/0167-6636(85)90012-2

5. Cowin, S. C., & Hegedus, D. H. (1976). Bone remodeling I: theory of adaptive elasticity. *Journal of Elasticity, 6*(3), 313-326. https://doi.org/10.1007/BF00041724

6. Engel, G. S., Calhoun, T. R., Read, E. L., et al. (2007). Evidence for wavelike energy transfer through quantum coherence in photosynthetic systems. *Nature, 446*(7137), 782-786. https://doi.org/10.1038/nature05678

7. Eringen, A. C. (1999). *Microcontinuum Field Theories: I. Foundations and Solids.* Springer-Verlag.

8. Hore, P. J., & Mouritsen, H. (2016). The radical-pair mechanism of magnetoreception. *Annual Review of Biophysics, 45*, 299-344. https://doi.org/10.1146/annurev-biophys-032116-094545

9. Huebsch, N., & Mooney, D. J. (2009). Inspiration and application in the evolution of biomaterials. *Nature, 462*(7272), 426-432. https://doi.org/10.1038/nature08601

10. Kinsey, L., Huizen, A. V., & Beane, W. (2023). Weak magnetic fields modulate superoxide to control planarian regeneration. *Frontiers in Physics, 10*, 1086809. https://doi.org/10.3389/fphy.2022.1086809

11. Kominis, I. K. (2015). The radical-pair mechanism as a paradigm for the emerging science of quantum biology. *Modern Physics Letters B, 29*(supp01), 1530013. https://doi.org/10.1142/S0217984915300136

12. Lambert, N., Chen, Y.-N., Cheng, Y.-C., Li, C.-M., Chen, G.-Y., & Nori, F. (2013). Quantum biology. *Nature Physics, 9*(1), 10-18. https://doi.org/10.1038/nphys2474

13. Marais, A., Adams, B., Ringsmuth, A. K., et al. (2018). The future of quantum biology. *Journal of the Royal Society Interface, 15*(148), 20180640. https://doi.org/10.1098/rsif.2018.0640

14. Mohseni, M., Rebentrost, P., Lloyd, S., & Aspuru-Guzik, A. (2008). Environment-assisted quantum walks in photosynthetic energy transfer. *Journal of Chemical Physics, 129*(17), 174106. https://doi.org/10.1063/1.3002335

15. Place, E. S., Evans, N. D., & Stevens, M. M. (2009). Complexity in biomaterials for tissue engineering. *Nature Materials, 8*(6), 457-470. https://doi.org/10.1038/nmat2441

16. Plenio, M. B., & Huelga, S. F. (2008). Dephasing-assisted transport: quantum networks and biomolecules. *New Journal of Physics, 10*(11), 113019. https://doi.org/10.1088/1367-2630/10/11/113019

Received: oct 02 ,2025 revised 28 oct 2025,

accepted 20 nov 2025, publication 26 Dec 2025

Volume 38 No. 12s 2025,

ISSN: 1311-1728 (printed version); ISSN: 1314-8060 (on-line version)

17. Prendergast, P. J., Huiskes, R., & Søballe, K. (1997). Biophysical stimuli on cells during tissue differentiation at implant interfaces. *Journal of Biomechanics, 30*(6), 539-548. https://doi.org/10.1016/S0021-9290(96)00140-6

18. Scala, I., Rosi, G., Nguyen, V.-H., Imperadori, S., Auffray, N., & Della Corte, F. (2024). Bone remodelling: a micromechanics-based continuum approach. *Meccanica, 59*, 1179-1195. https://doi.org/10.1007/s11012-024-01774-1

19. Schlosshauer, M. (2019). Quantum decoherence. *Physics Reports, 831*, 1-57. https://doi.org/10.1016/j.physrep.2019.10.001

20. Schrödinger, E. (1944). *What is Life? The Physical Aspect of the Living Cell.* Cambridge University Press.

21. Scrutton, N. S., & Hay, S. (2020). Proton-coupled electron transfer in enzymatic reactions. *Chemical Communications, 56*(55), 7637-7650.

22. Stuart, M. A. C., Huck, W. T. S., Genzer, J., et al. (2010). Emerging applications of stimuli-responsive polymer materials. *Nature Materials, 9*(2), 101-113. https://doi.org/10.1038/nmat2614

23. Yukawa, H., Kono, H., Ishiwata, H., Igarashi, R., Takakusagi, Y., Arai, S., Hirano, Y., Suhara, T., & Baba, Y. (2025). Quantum life science: biological nano quantum sensors, quantum technology-based hyperpolarized MRI/NMR, quantum biology, and quantum biotechnology. *Chemical Society Reviews, 54*(7), 3293-3322. https://doi.org/10.1039/D4CS00650J

24. Zurek, W. H. (2003). Decoherence, einselection, and the quantum origins of the classical. *Reviews of Modern Physics, 75*(3), 715-775. https://doi.org/10.1103/RevModPhys.75.715

Received: oct 02 ,2025 revised 28 oct 2025,

accepted 20 nov 2025, publication 26 Dec 2025